IBIS/PICsIT Instrument Specific Software Scientific Validation Report

Luigi Foschini
INTEGRAL – IBIS Team
Istituto di Astrofisica Spaziale e Fisica Cosmica (IASF) del CNR
Sezione di Bologna, Italy

Version 2.0

February 2, 2004

	Revision History
v 1.0	First version for first software release of March 2003.
28/02/2003	
v 1.1	Update for the intermediate software release of May 2003.
30/04/2003	Early analysis of Cyg X–1, cleaning of cosmic–ray induced events,
	improvement of the position accuracy, comparison with ECOE data.
v 1.2	Update for OSA 3 release.
27/10/2003	Crab in rev 102; automatic source location; timing analysis.
	Some error corrected. Removed the non–standard analysis section.
v 2.0	General reshape of the document style. Update for OSA 3.1 release.
02/02/2004	Updated the discussion on the uniformity maps and the inclusion of GTI.

1 Introduction

This report summarizes the scientific performances and reliability of the Instrument Specific Software (ISSW) of the PICsIT detector layer of the IBIS imager aboard INTEGRAL. The executables analysed here, together with their Instrument Configuration (IC) files, are those delivered by the IBIS Team to the ISDC for the integration in the Off–line Scientific Analysis (OSA) software package version 3.1 released by the ISDC to the public by January 2004. An equivalent report on the IBIS/ISGRI ISSW is provided in a separate document by A. Goldwurm et al. (IBIS/ISGRI Instrument Specific Software Scientific Validation Report).

The basic concepts of the scientific analysis of the IBIS telescope are described in Goldwurm et al. (2001, 2003), while more detailed technical information about the pipelines, data structures, tools, and complementary modules can be found in the documents *Introduction to INTEGRAL Data Analysis* (ISDC/OSA–INTRO), *ISDC Data Repository Organization* (ISDC/TEC013), and *IBIS Analysis User Manual* (ISDC/OSA–UM–IBIS).

This report provides a preliminary evaluation of the scientific performances of the IBIS/PICsIT software according to the tests performed so far. Further tests will be available in the next versions of the present document.

2 The IBIS/PICsIT data analysis

2.1 General concepts

The general purpose in the data analysis of astronomical instruments can be basically divided into two parts: the first, based on the analysis of images, is to measure the celestial coordinates, the spatial structure (extended or point–like sources), and the photometry of the source. The second, related to the study of the spectra, is to measure the flux and energy of emission/absorption lines, and the characteristics of the continuum. The measuring process adds several effects that contribute to modify the original image or spectrum. Therefore, it is necessary to operate corrections to the data in order to obtain an image/spectrum that is as much as possible consistent with the original one. Despite the differences depending on the instrument used in the observation, from a purely conceptual point of view, it is necessary to solve an inverse problem with distribution functions. In other words, by assuming for the sake of simplicity a monodimensional case, we have to solve the following integral equation of Fredholm of the first kind:

$$\phi(x) = \int \psi(z) K(x,z) dz \tag{1}$$

where ϕ is the observed density of probability function, while ψ is the corresponding original density of probability fuction that we want to restore. K is the kernel of the integral equation and represents the measuring process, including the effects of the measuring errors in the observed distribution. The kernel is called *point–spread function* (PSF) in the images, while it is called *line–spread function* (LSF) in the spectra. ϕ, ψ, and K are all non–negative functions, since they are connected with the density of the incoming photons.

The basic problem of the astronomical software is therefore "to clean" the PSF or LSF from all the systematic errors (including those of calibrations), before to proceed to the inversion of the integral equation. At the end of the correction ("cleaning") process, the kernel should contain only the statistical errors intrinsic to the measuring process. For example, in the case of a gaussian distribution with variance σ^2, the kernel is:

$$K(x,z) = \frac{1}{\sigma\sqrt{2\pi}} \exp \frac{-(x-z)^2}{2\sigma^2} \tag{2}$$

Depending on the type of instrument, there are different types of corrections. A system for astronomical data processing can be divided into three main steps, which in turn can be divided into sub–steps. The first step (**Level 0**) is the *preprocessing* level, where the telemetry coming from the satellite is unpacked and converted into a standard format (FITS) (see in the ISDC Technical Document section[1]). The basic data structure (RAW and PRP) is built, together with the On–Board Time (OBT) information, and the division into Science Windows (ScW) is set up (see ISDC/TEC013 for more details).

It is worth noting that, in the case of IBIS/PICsIT, there is also an on–board processing of the data before the Level 0, performed by the Hardware Event Preprocessor of IBIS (HEPI). This is necessary because of the limited telemetry available on–board the INTEGRAL satellite and the high count rate of background (≈ 3500 c/s) in the IBIS/PICsIT energy range ($0.17 - 10$ MeV). Therefore, HEPI performs a preliminary processing of the event list (containing the position y, z of the pixel, the channels $0 - 1023$, and the time information), before to send it to the ground. The corrections are: equalization by applying the gain and offset values of the HEPI look–up tables (LUT), conversion from channels to energy to reconstruct the multiple events, integration of events into histograms to save telemetry. The histograms are divided into two types: one (*spectral imaging*) is a data cube of $256 \times 64 \times 64$, containing still the full spatial information (64×64 pixel) and a moderate energy resolution (from the original 1024 to 256 channels). The integration time of a single histogram is generally corresponding to the duration of one ScW (≈ 2000 s), resulting in a loss of time information. Therefore, to perform time study, the other type of histogram (*spectral timing*) is designed to keep time resolution down to 1 ms, but with a great loss of energy resolution (from 1024 to 8 channels), and without spatial information. The combination of the *spectral imaging* and *spectral timing* is called *standard mode*. It is worth noting that IBIS/PICsIT can download directly the event list, without the integration on–board (*photon–by–photon* mode PPM), but with great consumption of telemetry. Therefore, with the exception of some observations of calibration, IBIS/PICsIT works only in standard mode, by producing spectral imaging histograms for single and multiple events, and histograms in spectral timing (default 4 energy bands and 2 ms of time resolution). More details on IBIS/PICsIT on–board processing are available in the IBIS User Manual, Issue 5.1.

Once the basic data structure is set up, there is the correction step (**Level 1**) where the instrument dependent corrections are applied. In this level, the OSA pipeline starts to work and perform the sublevels COR, DEAD, GTI, BIN_I/BIN_S, BKG_I/BKG_S. The specific corrections for IBIS/PICsIT are:

1. the intrinsic deadtime of the detector, that is the time during which it is not possible to process any event, since the detector is devoted to the processing of another event;
2. additional deviations from the on–board tables of gain and offset (only for PPM), and conversion from channels to energy;
3. filtering of the events according to the Good Time Intervals (GTI); for PPM only;
4. correction of partially downloaded histograms (for standard mode only);
5. correction for detector non–uniformities and subtraction of the background.

When the data are cleaned from background and corrected for instrumental effects, it is possible to move to the third level (**Level 2**), where the creation of images, spectra, and lightcurves is done (sublevels CAT_I/CAT_S, IMA/IMA2, SPE, LCR). The shadowgrams, produced in the previous level, are deconvolved according to the algorithms explained in Goldwurm et al. (2001, 2003), and the search for known sources is done, starting from a general catalog (Ebisawa et al. 2003). The attitude values of right

[1] Available at `http://isdc.unige.ch/index.cgi?Documents+doctec`.

ascension and declination obtained from the star tracker are referred to IBIS/PICsIT, by using a rotation and traslation (IBIS/PICsIT and the star tracker are not aligned). Moreover, the deconvolved image is projected into the sky with the gnomonic projection (TAN, cf Calabretta & Greisen 2002). The standard products of the source detection, performed on the sky images, is composed of the source coordinates and errors (in celestial coordinates and in pixels), the flux and its error (in counts per second), and the significance.

In the part of the extraction of the spectra, whose algorithms are still described in the seminal papers by Goldwurm et al. (2001, 2003), two IC files are of extreme importance. The first, named Auxiliary (or Ancillary) Response File (ARF) contains the information about the effective area of the detector as a function of the photon energy. The second IC file is named Redistribution Matrix File (RMF) and contains the information necessary to convert the counts into photons. This part is not yet included into OSA, since the RMF/ARF files are still missing.

The lightcurves are generated by using the spectral timing data, and therefore they are simply the count rates versus time for the whole detector. The deadtime and barycentric corrections are applied. The extraction of lightcurves for single point sources is not yet implemented, since it can be done only in PPM.

The output of the OSA pipeline can be analysed by means of the common software for high–energy astrophysics (e.g. Xspec, DS9, Xronos, ...).

2.2 General description of the executables

The IBIS/PICsIT–ISSW delivered to date for the Scientific Analysis of the PICsIT data include:

- `ibis_pics_deadtime` (v 2.2, 8 January 2004, DEAD level):
  to calculate the intrinsic deadtime of each semimodule of the detector. It is based on the use of a specific IBIS/PICsIT housekeeping, the *livetime counter*, that provides already the effective live time for each semimodule every 8 seconds.

- `ip_ev_correction` (v 1.6, 14 November 2002, COR level):
  to perform a correction of gain and offset variations in addition to those performed on board by HEPI. It is for data obtained in photon–by–photon mode. It is strilctly linked with the IC data structure PICS–ENER–MOD, containing the average gain, offset, and the deviations from these values pixel by pixel. The latest version of PICS–ENER–MOD is dated 30 October 2002 and was built by using the data in the IBIS Scientific Performance Report (IBIS Calibration Team, 2002). A new table in under preparation, to make full use of the analysis of the in–flight behaviour (Malaguti et al. 2003a). The exectuable is now stable and working. The only expected changes concerns the IC file, that should be updated with in flight data.

- `ip_ev_shadow_build` (v 2.3, 14 January 2004, BIN_I/BIN_S level):
  to perform the building of the shadowgrams and the efficiency maps (dimensions 64×64) from data in photon–by–photon mode, according to energy bands or time bins selected by the user. The events are cleaned from the spurious events induced by cosmic-rays and selected according to the available table of Good Time Intervals (GTI), which in turn are generated by another set of executables made by ISDC. See Sect. 3.2 for more details.

- `ip_si_shadow_build` (v 2.7, 10 June 2003, BIN_I/BIN_S level):
  to perform the building of shadowgrams and the efficiency maps (dimensions 64×64) from the data in standard mode (spectral imaging). If histograms are not complete, the executable returns simply a warning, but it continues the analysis. The missing pixels will be trated as killed pixels.

- `ip_shadow_ubc` (v 2.4, 25 February 2003, BKG_I/BKG_S level):
  to perform the correction for background and detector non–uniformities. The output shadowgrams are also expanded to take into account the gaps between modules (from 64×64 to 65×67). The gaps and the killed pixels are filled with a mean value. There is also a variance map, calculated starting from the statistical variance of the detector counts and updated according to the correction performed (filled pixels, background subtraction, and so on...). The executable is linked with the following IC data structures: PICS–SBAC–BKG (background maps for single events), PICS–MBAC–BKG (background maps for multiple events), PICS–SUNI–BKG (detector non–uniformities for single events), and PICS–MUNI–BKG (detector non–uniformities for multiple events). See Sect. 3.1 for details.

- `ip_skyimage` (v 2.5, 07 January 2004, IMA2 level):
  it performs the deconvolution and sky image reconstruction by means of the algorithm described by Goldwurm et al. (2003). The executable is working, producing a basic deconvolved sky image, variance, and significance maps. For staring observation, it is possible to integrate the shadowgrams before the deconvolution and the automatic source location. For observations with dithering pattern, it is not possible to sum the shadowgrams before the deconvolution. Therefore, this module perform the basic deconvolution for every ScW. The output images can be summed to generate mosaics with other tools, available in the OSA (see *IBIS Analysis User Manual*), or from other developers. A module for mosaic and source detection in dithering specific for IBIS/PICsIT will be available in the OSA 4.0 (SCREW 1363). See Sect. 4 for details.

- `ip_st_lc_extract` (v 2.2, 11 September 2003, LCR level):
  it performs the extraction of the lightcurve of the whole detector from the spectral timing data. The barycentric correction is applied, by using the library DAL3AUX. The executable is stable and working. The output files are in compliance with OGIP standards([2]).

It is worth noting that the IBIS/PICsIT ISSW makes use of other executables when inserted into the IBIS pipeline (creation and merging of GTI, Catalog Extraction, and so on...). These executables have been developed by ISDC people and are not analysed here directly, although the proper working of these modules is essential to have the full software package.

More details on some single items are in the following sections.

3 The correction for background

3.1 Maps

IBIS/PICsIT operates in an energy region dominated by the background (that is also higher than expected from numerical models – cf Ferguson et al. 2003), where we expect that the source counts are of the order of 1% of the global counts detected. This means that the background correction is of paramount importance for the instrument capabilities.

The photons interacting with IBIS/PICsIT are distributed in a non–uniform way, because of several reasons (see Natalucci et al. 2003 for more details). The main effect is to produce an enhancement of counts at the edges of the modules and semimodules. Therefore, before to perform the deconvolution, it is necessary to flatten the detector non-uniformities. Presently, a first set of maps is available for the ISSW (`pics_suni_bkg_0004.fits` and `pics_muni_bkg_0003.fits`). These maps were produced by Lorenzo Natalucci of the IBIS Team, by means of MonteCarlo simulations: the shadowgrams produced by simulating the exposure of IBIS/PICsIT (in the energy range 170 keV - 10 MeV) to a source with $\Gamma = 2$.

[2] See http://heasarc.gsfc.nasa.gov/docs/heasarc/ofwg/ofwg_recomm.html

Then, a set of maps with the standard energy bands (see Table 1) has been produced and delivered to the ISDC. First tests have shown that these maps produce a negligible effect in the significance distribution (Fig. 1), that remains still a bit far from a purely gaussian distribution centered on zero and with a tail in the positive part, if any source is present in the FOV.

The background maps (`pics_sbac_bkg_0004.fits` and `pics_mbac_bkg_0005.fits`) have been prepared from the empty field observation of the revolution 38. The map for single events has an exposure of 13 ks, while that of multiple events has an exposure of 9 ks. *The present maps for uniformity and background correction are only a first approximation and more detailed maps are still needed.* Particularly, it is necessary to study the small, medium, and large scale contributions to the background structure, and to separate from the aberrations of the gamma–ray camera and detector. An interesting analysis of the background of a similar gamma–ray instrument, SIGMA onboard GRANAT, is presented in Bouchet et al. (2001).

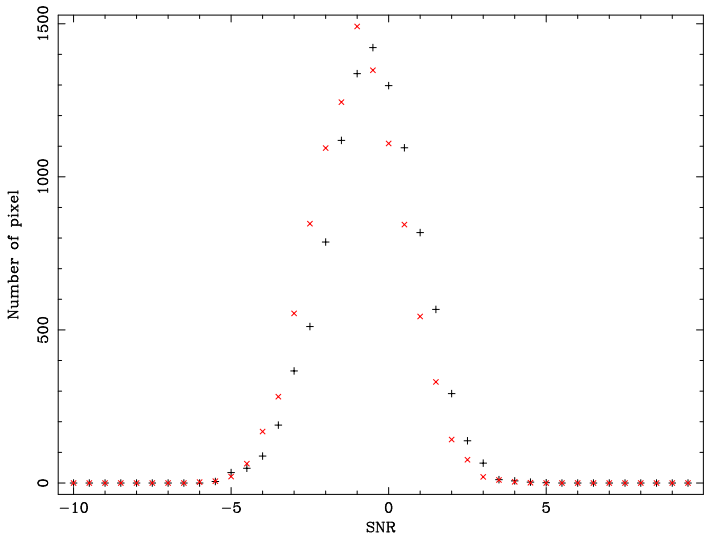

Figure 1: Significance distribution in the pixels during the Crab observation in staring (revolution 39, band $203-252$ keV, about 100 ks exposure). The distribution in the standard observation (no uniformity map) is shown with +, while × indicates the distribution after the application of Natalucci's uniformity maps.

One set of default energy bands has been created to have the best source statistics, with the lowest possible contamination from background or other events, such as the cosmic–rays induced events (see Segreto et al. 2003). These energy bands, prepared by G. Di Cocco and G. Malaguti, are shown in Table 1.

Table 1: PICsIT Energy Bands. Columns: (1) Channel number in photon–by–photon mode; (2) Channel number in standard mode; (3) Energy [keV].

Channels PPM (1)	Channels Standard (2)	Energy (3)	Channels PPM (1)	Channels Standard (2)	Energy (3)
Single Events			Multiple Events		
$29-35$	$10-16$	$203-252$	$24-31$	$5-12$	$336-448$
$36-46$	$17-27$	$252-329$	$32-46$	$13-27$	$448-658$
$47-64$	$28-41$	$329-455$	$47-74$	$28-46$	$658-1050$
$65-94$	$42-56$	$455-655$	$75-130$	$47-74$	$1050-1834$
$95-150$	$57-84$	$655-1057$	$131-254$	$75-136$	$1834-3570$
$151-262$	$85-140$	$1057-1841$	$255-464$	$137-187$	$3570-6510$
$263-509$	$141-196$	$1841-3570$	$465-679$	$188-229$	$6510-9520$
$510-929$	$197-254$	$3570-6510$	$680-929$	$230-254$	$9520-13020$

Presently the executable contains two ways to rescale the background maps: according to the time of exposure and to the average value of counts. Although a more detailed study is necessary, it appears that the average value scaling could give better results. The distribution of significance values in the pixels of the field of view during the Crab observation of calibration is generally a gaussian, with a peak close to 0. A residual of $\pm 0.2\sigma$ is sometimes present. This systematic error will be corrected in the future versions of the software.

3.2 Cosmic–ray induced events

Since the beginning of the in–flight operations, it was clear that there were spurious events contaminating the detector in addition to the backgroud and source events([3]). The cause was identified in cosmic–ray induced events, that are roughly the 10% of the total events and affect mainly the energy bands below 300 keV (Segreto et al. 2003, see also Natalucci 2003). As underlined by Natalucci (2003) these fake events can significanly affect the performances of PICsIT. However, it is possible to perform a cleaning only in photon–by–photon mode. In standard mode, it is possible to perform only an *a posteriori* correction: when the pixel counts are higher than a constant multiplied by the average count values, i.e. $counts > k \cdot average$ (see Fig. 2), then it is assumed that this abnormal high value is due to a cosmic–ray induced event and the pixel value is reset to the mean value. First tests showed a certain effectiveness of this correction, although the random nature of this type of correction introduces strong fluctuations in the count rates and significances in the reconstructed sky images.

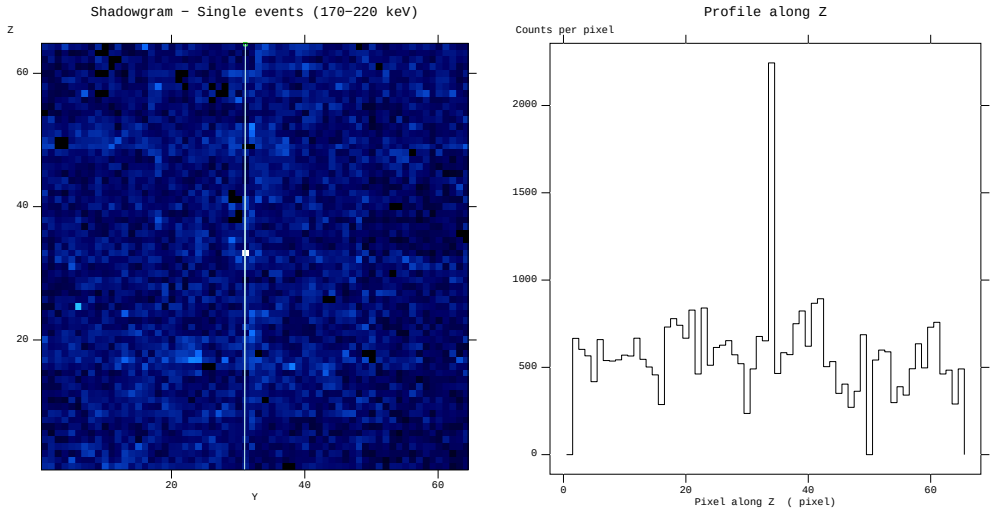

Figure 2: Effect of cosmic-rays induced events on the shadowgrams. The white pixels have an anomalous high count value. This example is taken from the data of revolution 24 in the energy band 170 – 220 keV; PICsIT was in photon–by–photon mode.

This hypothesis is confirmed by the analysis of photon–by–photon data: indeed, in this case, it was possible to develop an algorithm to delete from the photon list those events that can be identified as fake. After having isolated some of these "tracks", the photon list displayed series of photons "packed" in a very short time scale hitting a single pixel. Such "packets" are shown in Fig. 3, where fake events are emphasized in blue.

By removing these "packets" it is possible to obtain a cleaned shadowgram (Fig. 4), but – obviously – this is possible only when PICsIT is set to operate in photon–by–photon mode. Since the available telemetry is not sufficient for this type of mode, PICsIT works almost always in standard mode (i.e. with events

[3] See some nice animations by the IBIS Team in Tübingen at http://astro.uni–tuebingen.de/groups/integral/anim_gif/.

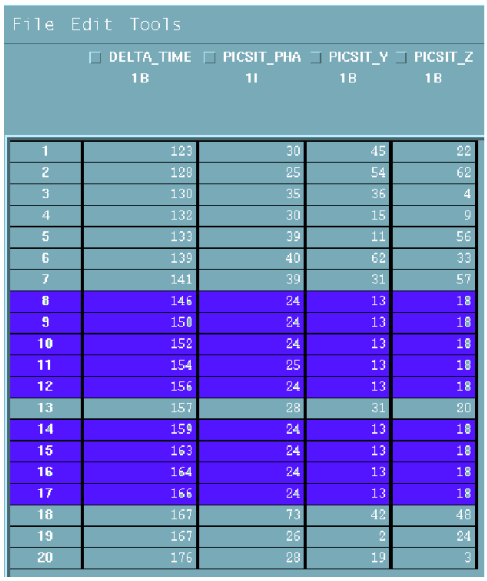

File Edit Tools

	DELTA_TIME 1B	PICSIT_PHA 1I	PICSIT_Y 1B	PICSIT_Z 1B
1	123	30	45	22
2	128	25	54	62
3	130	35	36	4
4	132	30	15	9
5	133	39	11	56
6	139	40	62	33
7	141	39	31	57
8	146	24	13	18
9	150	24	13	18
10	152	24	13	18
11	154	25	13	18
12	156	24	13	18
13	157	28	31	20
14	159	24	13	18
15	163	24	13	18
16	164	24	13	18
17	166	24	13	18
18	167	73	42	46
19	167	26	2	24
20	176	28	19	3

Figure 3: Identification in the photon list (single events) of fake events produced by cosmic–rays. Spurious events are emphasized in blue.

integrated onboard in histograms). In this mode, there is no possibility to act on the single photon and, therefore, it is possible only to operate the *a posteriori* correction described above.

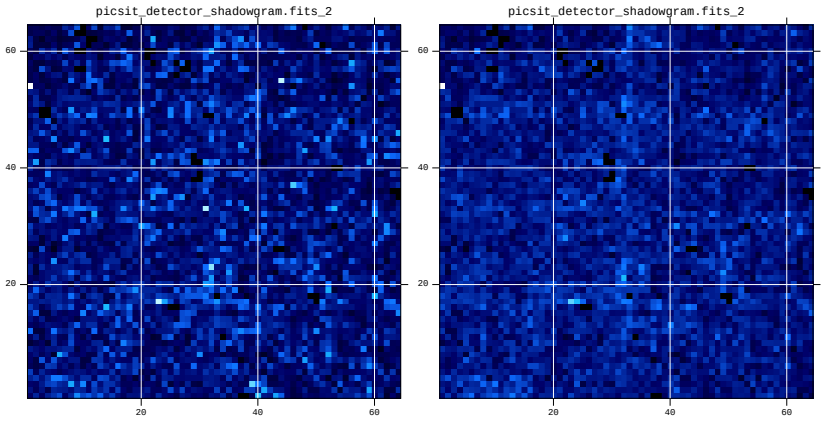

Figure 4: Effect of cosmic–rays induced events on the shadowgrams (photon–by–photon mode). (*left*) Normal shadowgram; (*right*) Cleaned shadowgram. After the cleaning, the bright pixels disappeared. The only bright pixel remained at the top left of the cleaned shadowgram is a well–known pixel that often is noisy. Data from revolution 14, energy band $170 - 250$ keV.

4 The sky image reconstruction

Here are shown some performances of the PICsIT ISSW. Details on the techniques of the deconvolution are available in Goldwurm et al. (2003).

4.1 Sky coordinates reconstruction

The sensitivity of PICsIT does not allow to see sources during a typical exposure of one ScW ($2-5$ ks). It is necessary to integrate the shadowgrams to obtain long exposures of the order of $10^4 - 10^5$ s. This resulted to be problematic in realizing a detailed and extensive study of misalignement. Therefore the correction for systematic effects in the sky coordinates reconstructions has been performed in two phases: during the first phase (from the PV phase to July 2003), the misalignement matrix was set equal to the identity and a correction was applied directly in the deconvolution module (`ip_skyimage`) in order to minimize the offset with the Crab position. During the second phase (from July 2003), the misalignement matrix of PICsIT has the same values of that of ISGRI, since it is expected that the misalignement of the two layers are equal (cf Walter et al. 2003). The correction performed in the deconvolution module has been removed from the version 2.4.

Table 2: Source position accuracy. Columns: (1) Source name; (2) Reference position (RA, Dec, J2000) from catalog or circulars; (3) PICsIT position (RA, Dec, J2000); (4) Offset [arcmin]. The position for PICsIT are taken in the $252-329$ keV energy band. The two positions for the GRB refers to that from the plain deconvolution (*Plain*) and that after the interpolation (*Int*).

Source	Reference Position	PICsIT Position	Offset
(1)	(2)	(3)	(4)
Cygnus X–1	$19:58:22;+35:12:06$	$19:58:08;+35:08:40$	$4.4'$
Crab Star	$05:34:32;+22:00:52$	$05:34:13;+21:55:48$	$6.8'$
Crab Star Int (*)		$05:34:33;+21:59:13$	$1.7'$
Crab Dith		$05:34:24;+22:01:20$	$1.9'$
Crab Off Ax		$05:34:17;+21:59:11$	$3.8'$
GRB 021125 Int	$19:47:56,+28:23:28$	$19:47:46,+28:17:14$	$6.6'$
GRB 021125 Plain		$19:47:34,+28:15:13$	$9.5'$

To date, only three sources are available to test the sky coordinates reconstruction: they are Cygnus X–1 and Crab – in the FCFOV – and GRB021125 – in the PCFOV – (Bazzano and Paizis 2002). The position of the Crab and Cygnus X–1 can be checked with the known catalog position, e.g. Simbad. For the GRB there can be the problem that the only position available with sufficient precision is that obtained with ISGRI (Gros and Produit 2002), the low–energy detector layer of IBIS, and there is the risk of self–reference. But the follow–up with other satellites of the GCN (GRB Coordinates Network) confirmed the position.

In the Table 2 are reported the positions found and the comparison with the other known coordinates. The positions marked with (*) is the output from the automatic source detection for staring observations and with the misalignement matrix of July 2003. All the others refers to the early phase, with the identity misalignement matrix and the correction in the deconvolution.

The three positions for the Crab are obtained from the staring observation during the revolution 39 (Crab Star, 77 ks), from dithering osbervation of the revolution 43 (Crab Dith, 132 ks), and from Crab off–axis of 0.5° from the revolution 44 (Crab Off Ax, 104 ks). The position for Cyg X–1 is obtained from the dithered observation of revolution 11 (80 ks).

The fact that PICsIT shows the best results in the energy band $252-329$ keV can be due to the fact that this band is sufficiently low to have enough photons, but also sufficiently high to be not so much affected by the cosmic–ray induced events.

It is worth noting that one pixel of PICsIT corresponds to about $10'$, so that an offset of $6.6'$ corresponds just to about half a pixel.

5 Imaging with the calibration sources

5.1 Crab

For the analysis with the Crab were selected the data from the revolution 39 (Crab on axis, staring, 77 ks), 43 (Crab on axis, dithering, 132 ks), and 44 (Crab off axis of 0.5°, dithering, 104 ks), and 102 (Crab on axis, dithering, 47 ks). The results are shown in the Table 3.

Table 3: PICsIT observations of the Crab during Rev. 39 (staring, on axis, 77 ks), Rev. 43 (dithering, on axis, 132 ks), Rev. 44 (dithering, off axis 0.5°, 104 ks), Rev. 102 (dithering, on axis, 47 ks). The columns indicate the energy band [keV], the count rate in the peak pixel [c/s] and the significance of the detection for each revolution.

	Rev 39		Rev 43		Rev 44		Rev 102	
Energy Band	Rate	σ	Rate	σ	Rate	σ	Rate	σ
$200 - 252$	2.5	7.4	1.5	5.9	3.1	5.7	1.8	2.7
$252 - 329$	2.2	11.0	2.1	10.0	2.6	8.0	2.3	6.4
$329 - 455$	1.3	7.1	1.2	6.5	1.4	5.0	1.1	3.5
$455 - 655$	0.7	4.4	0.6	3.3	0.6	3.0	0.6	2.3

Monte Carlo simulations by Del Santo et al. (2001) are available for comparison, although in different energy bands (Table 4).

Table 4: Monte Carlo simulations of PICsIT observations of the Crab. Columns: (1) Energy band [keV]; (2) Count rate [c/s].

Energy Band (1)	Rate (2)
$150 - 250$	10
$250 - 400$	4.6
$400 - 1000$	2.1

The best performances of PICsIT are obtained in the energy band $252 - 329$ keV, that is less affected by the cosmic–rays induced events and is in a range sufficiently low to detect enough photons. In the Fig. 5-7 are shown the significance maps of the observation at $252 - 329$ keV, the best detection, together with the radial profile.

Table 5: PICsIT normalized observations of the Crab during Rev. 39 (staring, on axis, 77 ks), Rev. 43 (dithering, on axis, 132 ks), Rev. 44 (dithering, off axis 0.5°, 104 ks). The columns indicate the energy band [keV] and the significance of the detection for each revolution. The significance has been rescaled to the 132 ks of exposure of rev 43.

	Rev 39	Rev 43	Rev 44
Energy Band	σ	σ	σ
$200 - 252$	9.6	5.9	6.4
$252 - 329$	14.3	10.0	9.0
$329 - 455$	9.2	6.5	5.6
$455 - 655$	5.7	3.3	3.4

The greatest differences in the count rates and significance (for observations in staring, dithering, off axis) occur just the band $203 - 252$ keV, where we expect that the impact of cosmic–ray induced events is still high and the *a posteriori* correction – the only available since PICsIT is operated in histogram mode – may not be too much accurate (see Sect. 3.2).

It is worth mentioning that during the observations of the calibration sources some tests of the photon-by-photon mode have been set up and performed, with special telemetry allocation to PICsIT (e.g.

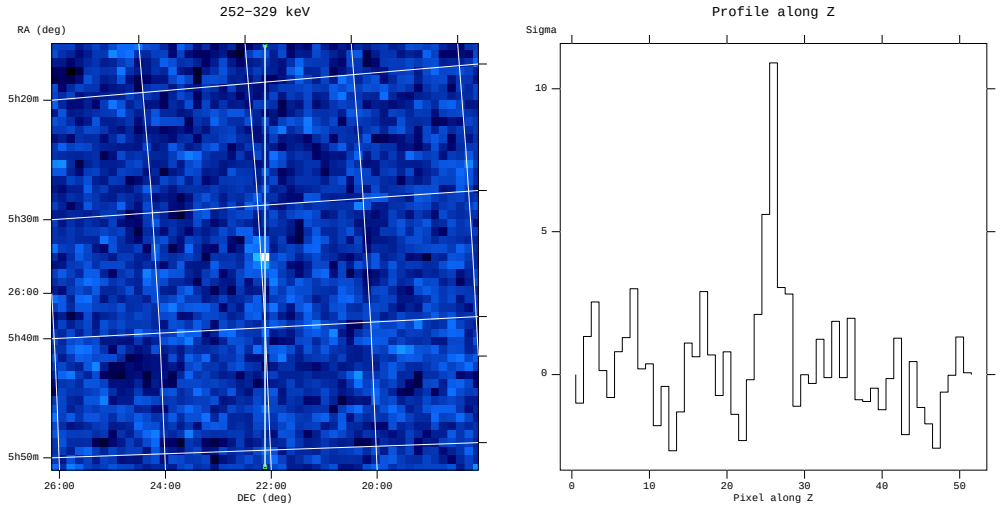

Figure 5: Crab observation during the rev 39 (staring, on axis, 77 ks). Significance map and profile in the energy band 252 – 329 keV.

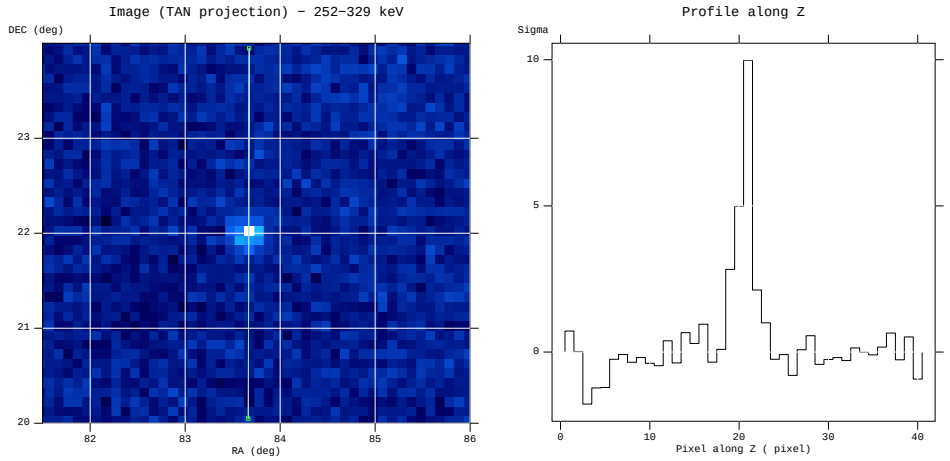

Figure 6: Crab observation during the rev 43 (dithering, on axis, 132 ks). Significance map and profile in the energy band 252 – 329 keV.

revolutions 39 and 40). However, despite this configuration, the limited telemetry budget resulted in a loss of about 80% of the pointing time. From an observation 100 ks long at the beginning of the revolution 40, the effective exposure is only 23 ks. An inspection of the GTI table and of the lightcurve revealed that the missing time was due to telemetry gaps.

In addition, we expect to have a degradation of the performances of the instrument when we change mode of observation (staring to dithering) or when we have the source off axis. Indeed, particularly during the 5×5 dither pattern, the source can be observed in the partially coded field of view, therefore in a region with less response than the fully coded field of view. To evaluate this effect, the three observations of the Crab (staring, dithering, dithering and off axis) have been normalized to the exposure of 132 ks (Table 5). Although it is expected that the value are a bit lower when passing from staring to dithering, since the mosaic performs an interpolation (pixels are not always perfectly aligned), this can account of only for a difference of 10%. Therefore, the greater differences shown in Table 5 are mostly due to other factors. This effect is still to be studied with more detailed tests.

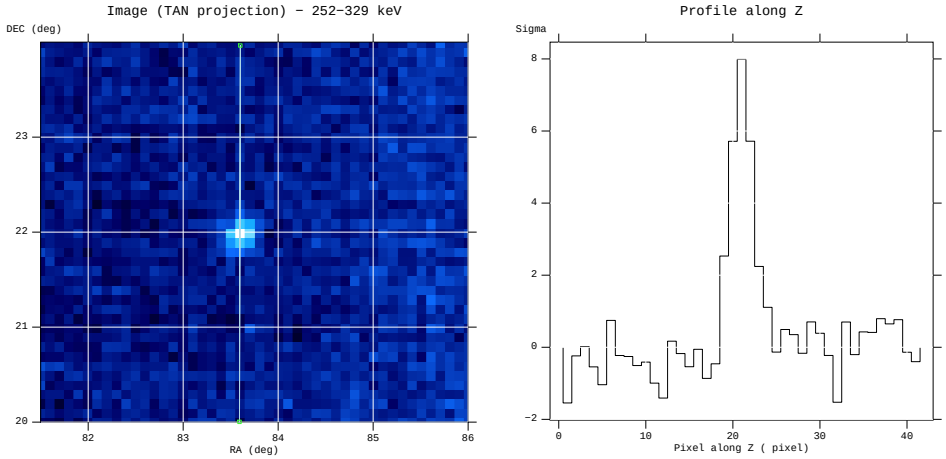

Figure 7: Crab observation during the rev 44 (dithering, off axis (0.5°), 104 ks). Significance map and profile in the energy band 252 – 329 keV.

5.2 Cygnus X–1

Soon after the launch of INTEGRAL (17 October 2002), it was not possible to observe the Crab, since it was too close to the Sun. Therefore, Cygnus X–1 was selected as calibration source. The first observations started during the revolution 11 and PICsIT was in standard mode. For other reasons, it was not possible to analyse immediately Cygnus X–1, but now – with the consolidated data – it is possible. To date the revolution 11 (80 ks, dithering) and 12 (13 ks, staring) have been analysed, with the detection of Cygnus X–1 in the first three energy bands of the observation in revolution 11. The 13 ks of the revolution 12 were not sufficient for a detection. The best detection is shown in Fig. 8. Since at that time there were several tests on the VETO configuration, the image is quite noisy, with fluctuations in the background. Nevertheless, the detection is clearly visible.

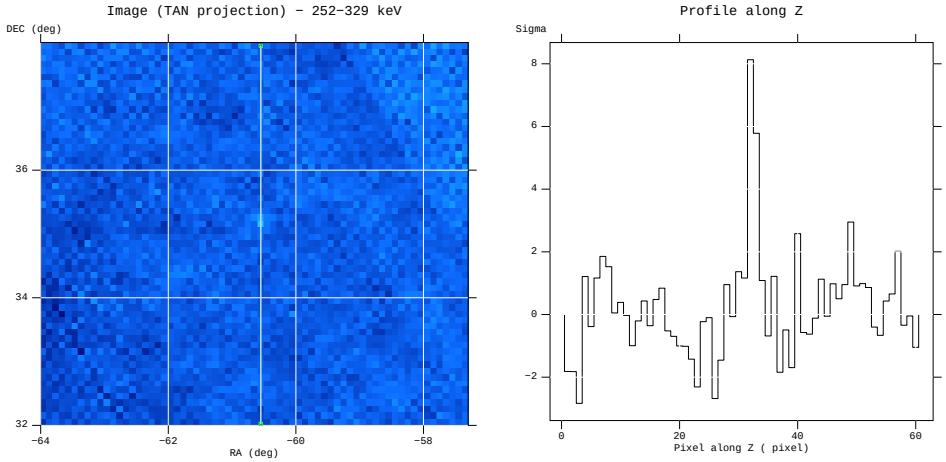

Figure 8: Cyg X–1 observed by PICsIT during the revolution 11 for 80 ks, dithering. Energy band 252 – 329 keV. Some background structures are clearly visible.

6 Timing

In February 2003, during the observation of the Crab, IBIS/PICsIT was set up to test the timing performances in the different modes of operation, i.e. photon–by–photon and spectral timing. Details on these observations and comparison with simultaneous observations with RXTE are published by Kuiper et al. (2003). The data analysed are from the revolutions 40 and 41, for a total of 345 ks (spectral timing, 1 ms time resolution), and from revolutions 39 and 40 in PPM. The Crab is detected at 16σ in spectral timing mode and the pulse shape is consistent with those from other instruments onboard INTEGRAL and RXTE. The bridge emission is expected given the energy range analysed ($260 - 364$ keV).

7 Known problems in OSA for PICsIT

1. Since the background subtraction is of fundamental importance for PICsIT detection capabilities, the energy band selection is strictly related to the background maps. In the current release, there is only one set of maps with fixed energy bands. Default values of the energy bins of PICsIT imaging have to be kept.

2. As the RMF are not available for PICsIT, you cannot run the BIN_S or the SPE step. It will stop with the error message:
   ```
   Error_2 2003-07-09T08:39:16 ibis_binning 5.2:  Could not find INDEX !
   status = -2104
   Error_1 2003-07-09T08:39:16 ibis_binning 5.2:  IC problem for category
   PICS-SRMF-GRP status -2104
   ```

3. If the first scw in an observation group is not a pointing, the PICsIT pipeline could finish without performing the deconvolution of the others scw. Please use only pointing scw.

Note: More informations on the in–flight performances of IBIS/PICsIT are available in the paper by Di Cocco et al. (2003). See also Malaguti et al. (2003b) for an analysis of the GRB021125.

Note: To make mosaics, it was used an executable originally developed by M. Revnivtsev to work on ISGRI data and modified by myself to use PICsIT images. With the kind permission of the author.

8 References

- Bazzano A., Paizis A., 2002, GCN1706
- Bazzano A., Bird A.J., Capitanio F., et al., 2003, A&A 411, L389
- Bouchet L., Roques J.P., Ballet J., Goldwurm A., Paul J., 2001, ApJ 548, 990
- Calabretta M.R., Greisen E.W., 2002, A&A 395, 1077
- Courvoisier T.J.-L., Beckmann V., Bourban G., et a., 2003, A&A 411, L343
- Del Santo M., Bazzano A., Bird A.J., et al., 2001, AIP Conference Proceedings **587**, 826.
- Di Cocco G., Caroli E., Celesti E., et al., 2003, A&A 411, L189
- Ebisawa K., Bourban G., Bodaghee A., et al., 2003, A&A 411, L59
- Ferguson C., Barlow E.J., Bird A.J., et al., 2003, A&A 411, L19
- Goldwurm A., Goldoni P., Gros A., et al., 2001, In: "Exploring the gamma–ray universe. Proceedings of the Fourth INTEGRAL Workshop", 4-8 September 2000, Alicante, Spain. Editor: B. Battrick, Scientific editors: A. Gimenez, V. Reglero, and C. Winkler. ESA SP–459, p. 497.
- Goldwurm A., David P., Foschini L., et al., 2003, A&A 411, L223
- Gros A., Produit N., 2002, GCN1714
- Kuiper L., Hermsen W., Walter R., Foschini L., 2003, A&A 411, L31
- IBIS Calibration Team, *Scientific Performance Report*, IN.IB.IAS.RP.008/02, March 2002.
- Malaguti G., Bazzano A., Bird A.J., et al., 2003a, A&A 411, L173
- Malaguti G., Bazzano A., Beckmann V., et al., 2003b, A&A 411, L307
- Natalucci L., Bird A.J., Bazzano A., et al., 2003, A&A 411, L209
- Segreto A., Labanti C., Bazzano A., et al., 2003, A&A 411, L215
- Walter R., Favre P., Dubath P., et al., 2003, A&A 411, L25